Polymer Journal, Vol. 20, No. 8, pp 627—638 (1988)

NMR Measurement of Identical Polymer Samples by Round Robin Method II. Reliability of Spin-Lattice Relaxation Time and Nuclear Overhauser Enhancement Factor

Riichirô CHÛJÔ, Koichi HATADA,* Ryozo KITAMARU,**
Tatsuki KITAYAMA,* Hisaya SATO,*** Yasuyuki TANAKA,***
Fumitaka HORII,** and Yoshio TERAWAKI*

Department of Polymer Chemistry, Tokyo Institute of Technology, Ookayama 2-chome, Meguro-ku, Tokyo 152, Japan
**Department of Chemistry, Faculty of Engineering Science, Osaka University, Toyonaka, Osaka 560, Japan*
***Institute for Chemical Research, Kyoto University, Uji, Kyoto 611, Japan*
****Department of Material Systems Engineering, Faculty of Technology, Tokyo University of Agriculture and Technology, Koganei, Tokyo 184, Japan*

(Received February 1, 1988)

ABSTRACT: ^{1}H and ^{13}C NMR spin-lattice relaxation times (T_1) and ^{13}C nuclear Overhauser enhancement (NOE) of radically prepared poly(methyl methacrylate) ($\bar{M}_n$=28500) in $CDCl_3$ were measured on 27 NMR spectrometers. Frequency range covered between 60 and 500 MHz for ^{1}H NMR. Precision of ^{1}H-T_1's of α-CH_3 and CH_2 protons was less than 5%. The ^{1}H-T_1's of all sorts of protons increased linearly with increasing resonance frequency. The standard deviations for ^{13}C-T_1's were larger than those for ^{1}H-T_1's and exceeded 10% in some cases. The T_1's of all carbons except for the carbonyl carbon increased with frequency. The contribution of chemical shift anisotropy to the relaxation of the carbonyl carbon became significant above 25 MHz. The protons and carbons in the sequence rich in meso dyad showed longer T_1's than those in the corresponding sequence rich in racemo dyad. The precision of NOE was as good as that of ^{13}C-T_1. The NOE's decreased as the observing frequency increased and particularly the NOE for the carbonyl carbon became almost unity at 100 and 125 MHz.

KEY WORDS ^{1}H NMR / ^{13}C NMR / Poly(methyl methacrylate) / Round Robin Method / Spin-Lattice Relaxation Time / Nuclear Overhauser Enhancement / Signal Intensity / Frequency Dependence / Precision / Accuracy /

Nuclear magnetic relaxation parameters give important information on molecular motion and have become more and more familiar to and inevitable for many NMR users after the Fourier transform (FT) method was introduced to NMR technology. The relaxation parameters are also of essential importance in adjusting data acquisition conditions in FT NMR measurement to obtain quantitative data. Research group on NMR, Society of Polymer Science, Japan (SPSJ), collected ^{1}H and ^{13}C NMR spectra of two identical samples, poly(methyl methacrylate) and solanesol, from a number of NMR spectrometers. The results of assessment on the reliability of chemical shift and signal intensity were reported previously.[1] Insufficient agreement in the ^{13}C signal intensity urged us to assess the

reliability of spin-lattice relaxation time (T_1) and nuclear Overhauser enhancement (NOE) factor which are required for proper setting of conditions of measurements. It is also important to know whether or not the precision of determination of these parameters allows us to treat them as one of the characteristics of a polymer.

In polymer science power spectrum or frequency dependence is very important to elucidate molecular motion. The measurement of frequency dependence is, therefore, quite familiar in dielectric and/or mechanical relaxation studies. Meanwhile, a similar measurement is impossible in NMR study with one NMR instrument. Cooperation of many researchers with different instruments makes it possible to make measurements.

In this series of cooperative project several non-members as well as SPSJ members*[1] were invited to participate. The data were collected from spectrometers whose observing frequencies ranged from 60 to 500 MHz for ^{1}H NMR and from 15 to 125 MHz for ^{13}C NMR. As a result, frequency dependences of T_1 and NOE were obtained for a very wide range of frequencies. This paper reports the results of the reliability and consistency of T_1 and NOE values for the PMMA sample. A preliminary analysis of the data has been made[2] and the details will be published in the near future.

EXPERIMENTAL

Poly(methyl methacrylate)

Preparation and characterization of the PMMA are described in the previous paper.[1] Mean values for triad tacticities determined by ^{1}H NMR spectroscopy and their standard deviations, σ, are

$$mm = 4.0\%, \quad \sigma = 0.9,$$
$$mr = 34.7\%, \quad \sigma = 1.0,$$
$$rr = 61.3\%, \quad \sigma = 1.5.$$

The molecular weights are;

$$\bar{M}_n\,(\mathrm{GPC}) = 27400,$$
$$\bar{M}_n\,(\mathrm{VPO}) = 28500,$$
$$\bar{M}_w\,(\mathrm{GPC}) = 58000.$$

Measurement

A 10 w/v% $CDCl_3$ solution of the PMMA was degassed and sealed under nitrogen into 5 mm o.d. (for ^{1}H NMR measurements) and 10 mm o.d. (for ^{13}C NMR measurements) NMR sample tubes. The test samples were distributed to collaborating test sites. One particular sample (sample No. 1) was circulated to several test sites to obtain data on exactly the same sample from different instruments. In addition, some collaborators made measurements on sample solutions prepared by themselves from the distributed solid PMMA to assess any effects of sample preparation conditions on the data.

A requested method of T_1 determination was the inversion–recovery method with a pulse sequence of $(180°\text{-}\tau\text{-}90°\text{-}t)_n$. The time delays, τ and t, executed had the following ranges:

*[1] S. Amiya (Kuraray Central Research Laboratory), T. Asakura (Tokyo University of Agriculture and Technology), K. Chikaishi (Sumitomo Chemical Co. Ltd.), Y. Goto (University of Tokyo), K. Hikichi (Hokkaido University), Y. Hirakida (Showa Denko K.K.), S. Hosoda (Sumitomo Chemical Co., Ltd.), M. Imanari (JEOL Ltd.), S. Itoh (Kyoto University), M. Kamachi (Osaka University), T. Kawamura (University of Tokyo), S. Kohjiya (Kyoto Institute of Technology), K. Lee (Osaka University), I. Nagoya (Asahi Chemical Industry Co.), Y. Oka (Mitsui Toatsu Chemicals, Inc.), T. Okada (Tosoh Corporation), M. Okumura (Toa Nenryo Kogyo Kabushikigaisha), T. Saito (Nippon Oil Company, Ltd.), T. Sei (Daicel Chemical Industries, Ltd.), T. Seimiya (Idemitsu Kosan Co.), T. Shiibashi (Japan Synthetic Rubber Co.), T. Shimamura (Nitto Technical Information Center Co., Ltd.), M. Shimoda (Nippon Zeon Co., Ltd.), Y. Takai (Osaka University), T. Usami (Mitsubishi Petrochemical Co.), K. Ute (Osaka University), T. Yonemitsu (Kyushu Sangyo University).

	τ	t
^{1}H-T_1	0.001—10 s	4—20 s
^{13}C-T_1 of α-CH_3 and CH_2	0.005—10 s	1—20 s
^{13}C-T_1 of other carbons	0.010—15 s	10—20 s

NOE was determined from the intensity ratio of each carbon signal in the completely decoupled spectrum and gated decoupled spectrum without NOE. The executed conditions for the ^{13}C NOE determination were as follows:

pulse repetition time,	20—25 s
number of scans,	1000—2048

RESULTS AND DISCUSSION

^{1}H Spin-Lattice Relaxation Times of PMMA

^{1}H-T_1's of the PMMA in $CDCl_3$ were determined from the spectra measured on 27 spectrometers, whose resonance frequencies ranged from 60 to 500 MHz. Individual T_1 data for α-CH_3 protons in rr and mr triads, CH_2 and OCH_3 protons are listed in Table I in the order of increasing resonance frequency. ^{1}H-T_1 values increased with increasing magnetic field strength. The values obtained at any fixed frequency scatter only slightly with few exceptions. Table II summarizes the mean values and standard deviations of ^{1}H-T_1's determined at each resonance frequency. The precisions for ^{1}H-T_1's of α-CH_3 and CH_2 protons are as good as 5%. These T_1 values can be regarded as characteristic data for the polymer as long as obtained under the specified conditions. ^{1}H-T_1 data for OCH_3 protons showed a little larger standard deviations, partly due to the long T_1 values. α-Methyl protons in mr triad showed longer ^{1}H-T_1 than those in rr triad at each resonance frequency. The results clearly confirm similar observations by several investigators.[3-9] In Figure 1, the mean values of ^{1}H-T_1's are plotted against the resonance frequency for the respective protons. As is clearly seen in this figure, the T_1 values linearly increase with increasing resonance frequency for each proton but the slope of the straight line is considerably small for the α-CH_3 protons compared to the others. As a result, the α-CH_3 protons exhibit shorter ^{1}H-T_1's than CH_2 protons at frequencies high-

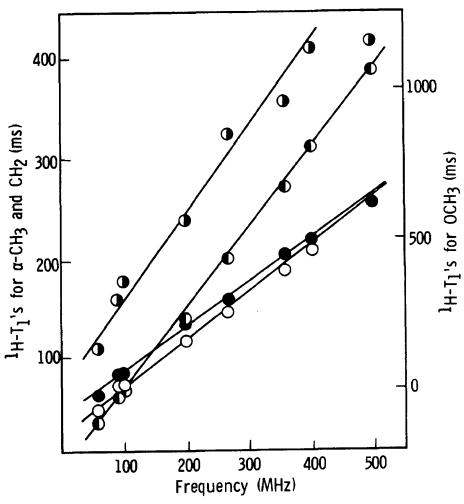

Figure 1. Frequency dependence of ^{1}H-T_1's of PMMA measured in $CDCl_3$ at 55°C: ○, α-CH_3 (*rr*); ●, α-CH_3 (*mr*); ◐, CH_2 (*rrr*); ◑, OCH_3.

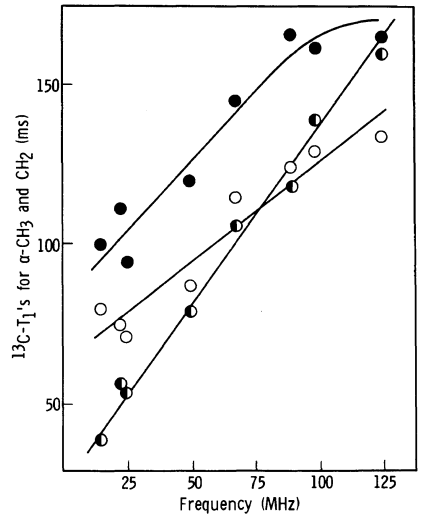

Figure 2. Frequency dependence of ^{13}C-T_1's for α-CH_3 and CH_2 carbons of PMMA measured in $CDCl_3$ at 55°C: ○, α-CH_3 (*rr*); ●, α-CH_3 (*mr*); ◐, CH_2.

Table I. Measurements of ^1H-T_1 (ms) for PMMA in $CDCl_3$ at 55°C by various spectrometers at different frequencies

Run[a]	Frequency (MHz)	Instrument	Temp (°C)	α-CH_3[b]		CH_2[b]	OCH_3[b]
				rr (0.87)	*mr* (1.03)	*rrr* (1.82)	(3.60)
A(1)	60	FX-60	55	50	60	40	140
B(1)	90	FX-90Q	55	75	89	67	281
X(1)	90	FX-90Q	55	68	79	62	306
Y(1)	90	FX-90Q	55	72	85	66	333
D(1)	100	FX-100	55	75	86	71	393
E(1)	100	FX-100	55	73	88	71	336
E(11)	100	FX-100	55	73	86	67	418
F(9)	100	FX-100	55	70	80	140	300
C(1)	100	FX-100	24	55	63	72	358
D(13)	100	FX-100	27	60	69	62	350
H(1)	200	FX-200	55	108	124	139	553
I(1)	200	XL-200	55	121	145	137	590
J(5)	200	XL-200	55	110	130	140	620
T(1)	200	FX-200	55	113	131	138	537
U(1)	200	XL-200	55	113	128	136	499
G(1)	200	FX-200	24	104	106	167	681
H(1)	200	FX-200	24	104	110	168	643
K(1)	270	GX-270	55	143	174	209	851
L(7)	270	GX-270	55	140	150	190	440
W(1)	360	AM-360	55	188	205	275	963
M(1)	400	GX-400	55	212	223	313	1367
M(1)	400	GX-400	55	207	221	316	1046
N(1)	400	GX-400	55	205	215	315	1130
O(8)	400	GX-400	55	205	224	320	1128
P(1)	400	GX-400	55	210	230	320	1130
Q(6)	400	GX-400	55	210	220	320	980
V(1)	400	GX-400	55	210	210	320	1150
R(1)	500	GX-500	55	257	253	392	730
R(1)	500	GX-500	55	249	253	339	1191
AA(1)	500	GX-500	55	266	265	410	1440
BB(1)	500	GX-500	55	264	269	414	1303

[a] Figures in parentheses denote sample numbers.
[b] Figures in parentheses denote chemical shifts measured at 55°C in $CDCl_3$.

er than 100 MHz, although the former has more nearest-neighbor protons than CH_2 protons. However, it seems very complicated to analyze these frequency dependencies in terms of simple models for the proton magnetic relaxation, because the previous ^1H NMR studies[3,5] revealed that cross relaxation significantly occurs among these protons.

Sample No. 1 was circulated to a number of test sites. No meaningful differences were ob-

Table II. ^{1}H-T_1's (ms) of PMMA measured in $CDCl_3$ at 55°C at different frequencies

Freq. (MHz)	n[a]	α-CH_3[b]		CH_2[b]	OCH_3[b]
		rr	*mr*	*rrr*	
60	1	50 (—)	60 (—)	40 (—)	140 (—)
90	3	72 (4.0)	84 (4.9)	65 (3.3)	307 (6.9)
100	3	74 (1.3)[d]	87 (1.1)[d]	70 (2.7)[d]	382 (9.0)[d]
100[c]	2	58 (4.3)	66 (4.5)	67 (7.5)	354 (1.1)
200	5	113 (3.9)	132 (5.4)	138 (1.0)	560 (7.5)
200[c]	2	104 (0)	108 (1.8)	168 (0.3)	662 (0.3)
270	2	142 (0.1)	162 (7.4)	200 (4.7)	851 (—)[e]
360	1	188 (—)	205 (—)	275 (—)	963 (—)
400	7	208 (1.3)	220 (2.7)	318 (0.9)	1133 (9.8)
500	4	259 (2.3)	260 (2.5)	389 (6.9)	1166 (20.5)

[a] Number of determinations.
[b] Figures in parentheses represent precision (%).
[c] Measurements were done at room temperature (24 and 27°C).
[d] The data F(9) were deleted.
[e] T_1 value of L(7) for OCH_3 was deleted.

Table III. Measurements of ^{1}H-T_1 (ms) at 55°C on the solution of PMMA in $CDCl_3$ prepared by each investigator

	Frequency (MHz)	α-CH_3		CH_2	OCH_3
		rr	*mr*	*rrr*	
D	100	74	87	70	398
E	100	76	91	72	286
U	200	111	125	136	443
H	200	109	129	128	553
M	400	204	218	321	1007

served in ^{1}H-T_1 values for different samples (Table I).

The data were also collected for sample solutions prepared at several test sites by each collaborator. The results obtained are shown in Table III and are in good agreement with the data shown in Table I. Therefore, as long as the preparation conditions of sample solution are specified, the T_1 data should not be altered substantially.

Possibly higher static magnetic fields are preferable for obtaining spectra with higher signal-to-noise (S/N) ratios. However, Figure 2 suggests that the increase in ^{1}H-T_1 at higher magnetic field strength requires setting a longer time as a repetition time between single rf pulses for the measurements. This would result in a decrease in practical S/N ratio obtainable within a limited period of time.

^{13}C Spin-Lattice Relaxation Times of PMMA

^{13}C-T_1's for the PMMA in $CDCl_3$ were measured at 55°C on 27 instruments, whose resonance frequency ranged from 15.0 to 125 MHz. The individual data are collected in Table IV. In Table V are summarized mean values and standard deviations at each resonance frequency. The deviations for ^{13}C-T_1's are larger than those for ^{1}H-T_1's and exceed 10% in some cases. Scattering of the data does not seem to be noticeably different with regard to types of carbon, though the deviation for OCH_3 is slightly larger than those of others similarly to the case of ^{1}H-T_1 for OCH_3. ^{13}C-T_1 values of α-methyl, quaternary and carbonyl carbons were determined for split signals due to tacticity. Carbons in the sequence rich in meso dyad generally showed larger ^{13}C-

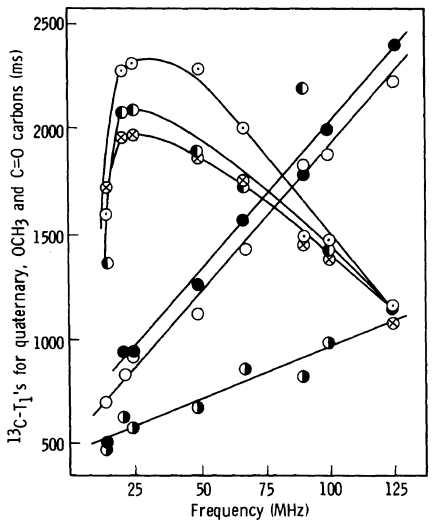

Figure 3. Frequency dependence of ^{13}C-T_1's for quaternary, OCH_3 and carbonyl carbons of PMMA measured in $CDCl_3$ at 55°C: ◑, OCH_3; ○, quaternary (*rr*); ●, quaternary (*mr*); ◐, carbonyl (*rrrm*); ⊙, carbonyl (*mmrr*+*rmrr*); ⊗, carbonyl (*rrrr*).

Table IV. Measurements of ^{13}C-T_1 (ms) for PMMA in $CDCl_3$ at 55°C using various spectrometers at different frequencies

Run[a]	Freq. (MHz)	Inst.	Temp (°C)	α-CH_3[b]		Quat. C[b]		OCH_3[b]	CH_2[b]	C=O[b]		
				rr (16.90)	*mr* (19.03)	*rr* (44.81)	*mr* (45.12)	(51.67)	*rrr* (54.25)	*mmrr*+*rmrr* (176.83)	*rrrr* (177.65)	*rrrm* (177.92)
A(1)	15	FX-60	55	80	100	700	460	460	40	1600	1720	840
B(1)	22.5	FX-90Q	55	85	109	870	990	550	57	2270	1990	2110
S(1)	22.5	FX-90Q	55	70	94	796	932	645	56	2311	1983	2019
X(1)	22.5	FX-90Q	55	79	113	759	890	634	58	2144	1892	1884
Y(1)	22.5	FX-90Q	55	63	127	826	938	661	51	2368	1888	2187
D(1)	25	FX-100	55	78	97	810	907	570	59	2085	1649	2218
E(1)	25	FX-100	55	61	75	809	923	561	49	2548	2012	1989
E(11)	25	FX-100	55	76	104	917	997	635	56	2590	2273	2213
F(9)	25	FX-100	55	70	100	1090	820	650	50	1990	1870	1850
C(1)	25	FX-100	24	32	35	500	230	210	30	1130	970	910
H(1)	50	FX-200	55	90	114	1179	1296	683	77	2221	1957	2012
I(1)	50	XL-200	55	85	129	908	927	524	85	1737	1751	1690
J(5)	50	XL-200	55	86	120	1150	1260	800	77	2160	1970	1860

T(1)	50	FX-200	55	96	127	1225	1347	801	81	2306	2037	2173
U(1)	50	XL-200	55	77	108	1216	1360	498	77	2944	1607	1663
G(1)	50	FX-200	24	56	93	1020	1040	532	71	1850	1680	1710
H(1)	50	FX-200	24	65	83	1055	1333	602	72	1755	1646	1553
K(1)	67.5	GX-270	55	115	145	1409	1554	861	105	2001	1740	1713
L(1)	67.5	GX-270	55	70	60	940	1030	670	40	1040	1130	1090
W(1)	90.6	AM-360	55	123	165	1820	1790	793	118	1450	1450	2200
M(1)	100	GX-400	55	139	165	1896	2116	956	141	1488	1386	1549
N(1)	100	GX-400	55	110	140	1795	1940	1435	130	1330	1260	1400
O(8)	100	GX-400	55	135	168	1831	1874	930	144	1372	1222	1275
P(1)	100	GX-400	55	140	170	1900	2040	880	140	1580	1400	1480
Q(6)	100	GC-400	55	140	180	1940	2020	950	140	1530	1380	1470
V(1)	100	GX-400	55	120	140	1860	1940	1150	140	1420	1290	1260
R(1)	125	GX-500	55	137	165	2253	2441	1116	167	1148	1121	1154
R(1)	125	GX-500	55	127	157	2149	2241	1071	146	1093	948	1083
AA(1)	125	GX-500	55	144	183	2400	2450	1470	167	1276	1129	1318
BB(1)	125	GX-500	55	128	158	2145	2317	970	146	1156	1101	1102

[a,b] Figures in parentheses denote sample numbers (a) and chemical shifts at 55°C in $CDCl_3$ (b).

Table V. ^{13}C-T_1 (ms) of PMMA measured in $CDCl_3$ at 55°C at different frequencies

Frequency (MHz)	n[a]	α-CH_3[b]		Quat. C[b]		OCH_3[b]	CH_2[b]	C=O[b]		
		rr	*mr*	*rr*	*mr*		*rrr*	*mmrr*+*rmrr*	*rrrr*	*rrrm*
15	1	80	100	700	460	460	40	1600	1720	840
22.5	4	74	111	813	938	623	56	2273	1938	2050
		(11.4)	(10.6)	(5.0)	(3.8)	(6.9)	(4.8)	(3.6)	(2.5)	(5.5)
25	4	71	94	907	912	604	54	2303	1951	2068
		(9.3)	(12.0)	(12.6)	(6.9)	(6.5)	(7.7)	(11.7)	(11.6)	(7.5)
50	5	87	120	1136	1238	661	79	2274	1864	1880
		(7.2)	(6.6)	(10.3)	(12.9)	(19.7)	(4.1)	(17.8)	(8.6)	(9.2)
50[c]	2	61	88	1038	1242	567	72	1803	1663	1632
		(7.4)	(5.7)	(1.7)	(16.3)	(6.2)	(0.7)	(2.6)	(1.0)	(4.8)
67.5[d]	1	115	145	1409	1554	861	105	2001	1740	1713
90.6	1	123	165	1820	1790	793	118	1450	1450	2200
100	6	129	161	1870	1988	973	139	1453	1323	1406
		(8.5)	(9.5)	(2.6)	(4.0)	(9.7)	(3.2)	(6.0)	(5.2)	(7.6)
125	4	134	165	2237	2362	1157	156	1168	1075	1164
		(5.2)	(6.3)	(4.6)	(3.7)	(16.3)	(6.7)	(5.7)	(6.9)	(7.9)

[a] Number of determinations.
[b] Figures in parentheses represent precision (%).
[c] Measurement was made at room temperature (24°C).
[d] The data L(7) were deleted.

T_1's than the corresponding carbons in the sequence rich in racemo dyad, as observed for ^1H-T_1 of α-CH_3 protons. Similar results on the ^{13}C-T_1 of PMMA have been reported by several investigators.[5,10-15] Figures 2 and 3 illustrate resonance frequency dependences of the mean values of ^{13}C-T_1. ^{13}C-T_1's for all carbons except for carbonyl carbon increase linearly with increasing resonance frequencies. The α-CH_3 carbon in rr triad shows longer T_1 than the CH_2 carbon in rrr tetrad at the lower frequencies but shorter T_1 at the higher frequencies, and the inversion in the order of magnitudes of ^{13}C-T_1 for α-CH_3 and CH_2 carbons occurs at the frequency between 67.5 and 90.6 MHz. Preliminary analyses have already shown that these frequency dependences of α-CH_3, CH_2, and OCH_3 carbons can be interpreted by molecular motional models in which the motion of the C–H internuclear vector is described in terms of three independent superposed motions with different correlation times.[2] The details of the explanation of difference in the frequency dependencies of the carbons will be published in this Journal.

^{13}C-T_1's for the carbonyl carbon decrease with increasing resonance frequencies above 25 MHz. The relaxation induced by chemical shift anisotropy is possible for the carbons in π-bond. The relaxation by this mechanism becomes important at higher magnetic field, since the contribution of chemical shift anisotropy to the relaxation rate is proportional to the square of the static magnetic field strength if the molecular tumbling rate is much larger than the resonance frequency.[16] The relaxation of the acetylenic carbons in 1,4-diphenylbutadiyne is a typical example of this case.[17] The great decrease in ^{13}C-T_1 of the carbonyl carbon in PMMA with increasing magnetic field indicates increasing contribution of the chemical shift anisotropy to the spin-lattice relaxation. To our knowledge, this is the first example of polymer system where the contribution of the chemical shift anisotropy to the relaxation was proved. Though the frequency dependency of ^{13}C relaxation was reported recently on poly(butyl methacrylate), the au-

Table VI. Measurements of ^{13}C-T_1 (ms) at 55°C on solutions of PMMA in $CDCl_3$ prepared by the investigators

	Frequency (MHz)	Instrument	α-CH_3		Quat. C		OCH_3	CH_2	C=O		
			rr	*mr*	*rr*	*mr*		*rrr*	*mmrr*+*rmrr*	*rrrr*	*rrrm*
E	25	FX-100	64	84	1011	888	564	51	2844	2186	2797
H	50	FX-200	80	115	1780	1290	680	79	2240	1970	2030
U	50	XL-200	90	112	1161	1356	667	82	1979	2031	1953

Table VII. Measurements of ^{13}C NOE for PMMA in $CDCl_3$ at 55°C by various spectrometers at different frequencies

Run[a]	Frequency (MHz)	Instrument	Temp (°C)	α-CH_3		Quat. C		OCH_3	CH_2	C=O		
				rr	*mr*	*rr*	*mr*		*rrr*	*mmrr*+*rmrr*	*rrrr*	*rrrm*
A(1)	15	FX-60	55	2.50	2.40	2.60	2.10	2.70	2.80	2.60	2.70	2.20
B(1)	22.5	FX-90Q	55	2.86	2.97	2.69	2.55	2.44	2.64	1.87	2.07	1.89
X(1)	22.5	FX-90Q	55	2.80	2.80	2.60	2.30	2.50	2.50	2.40	2.30	1.90
Y(1)	22.5	FX-90Q	55	2.26	2.11	2.42	2.22	2.23	1.92	2.03	2.20	1.69
D(1)	25	FX-100	55	2.73	2.67	2.50	2.63	2.53	2.61	2.32	2.07	2.14
E(1)	25	FX-100	55	2.77	2.85	2.45	2.62	2.44	2.74	2.01	2.26	2.07
E(11)	25	FX-100	55	2.65	2.76	2.49	2.58	2.68	3.11	2.63	2.43	2.39
F(9)	25	FX-100	55	2.73	2.52	2.43	2.36	2.42	2.42	2.24	2.18	2.25
C(1)	25	FX-100	24	2.75	2.75	1.95	1.95	1.89	2.09	1.62	1.62	1.62
H(1)	50	FX-200	55	2.75	2.73	2.34	2.18	2.18	2.57	1.97	1.72	1.66
I(1)	50	XL-200	55	2.57	2.72	2.04	2.24	2.17	2.05	1.68	1.61	1.92
J(5)	50	XL-200	55	2.52	2.39	1.86	2.04	1.91	1.88	1.45	1.44	1.36
T(1)	50	FX-200	55	2.60	2.64	2.13	2.12	2.11	2.08	1.83	1.72	1.66
U(1)	50	XL-200	55	2.80	2.76	2.20	2.26	2.21	2.05	1.72	1.60	1.47
G(1)	50	FX-200	24	2.18	2.33	1.67	1.89	1.87	1.74	1.41	1.36	1.39
H(1)	50	FX-200	24	2.24	2.38	1.83	1.82	1.75	1.85	1.45	1.42	1.38
K(1)	67.5	GX-270	55	2.51	2.48	2.04	1.95	2.01	1.97	1.49	1.37	1.27
L(7)	67.5	GX-270	55	2.10	2.35	1.72	1.72	1.74	1.69	1.21	1.20	1.18
W(1)	90.6	AM-360	55	2.07	2.03	1.98	1.97	1.66	1.71	1.59	1.33	1.33
M(1)	100	GX-400	55	2.44	2.32	1.77	1.82	1.73	1.77	1.19	1.17	1.18
N(1)	100	GX-400	55	2.03	2.28	1.62	1.69	1.62	1.59	1.06	1.01	1.04
P(1)	100	GX-400	55	1.80	1.90	1.60	1.60	1.50	1.50	1.10	1.00	1.00
Q(6)	100	GX-400	55	2.20	2.24	1.76	1.76	1.70	1.71	0.99	1.07	1.07
V(1)	100	GX-400	55	2.24	2.26	1.66	1.87	1.68	1.59	1.13	1.09	1.23
R(1)	125	GX-500	55	2.20	2.30	1.80	1.80	1.70	1.80	1.30	1.10	1.30
R(1)	125	GX-500	55	2.01	2.02	1.51	1.51	1.38	1.42	1.00	1.00	1.01
AA(1)	125	GX-500	55	2.20	2.40	1.70	1.30	1.60	1.70	1.10	1.10	1.10
BB(1)	125	GX-500	55	2.23	2.49	1.69	1.63	1.60	1.63	1.04	1.07	1.06

[a] Figures in parentheses denote sample numbers.

Table VIII. ^{13}C NOE of PMMA measured in $CDCl_3$ at 55°C at different frequencies

Frequency (MHz)	n[a]	α-CH_3[b]		Quat. C[b]		OCH_3[b]	CH_2[b]	C=O[b]		
		rr	*mr*	*rr*	*mr*		*rrr*	*mmrr*+*rmrr*	*rrrr*	*rrrm*
15	1	2.80	2.40	2.60	2.10	2.70	2.80	2.60	2.70	2.22
22.5	3	2.64	2.63	2.57	2.36	2.39	2.35	2.10	2.19	1.83
		(10.2)	(14.3)	(4.5)	(5.9)	(4.8)	(13.2)	(10.5)	(4.5)	(5.4)
25	4	2.72	2.70	2.47	2.55	2.52	2.72	2.30	2.24	2.21
		(1.6)	(4.5)	(1.1)	(4.4)	(4.1)	(9.2)	(9.8)	(5.8)	(5.5)
25[c]	1	2.75	2.75	1.95	1.95	1.89	2.09	1.62	1.62	1.62
50	5	2.65	2.65	2.11	2.17	2.12	2.13	1.73	1.62	1.61
		(4.1)	(5.1)	(7.6)	(3.7)	(5.1)	(10.9)	(9.8)	(6.6)	(11.7)
50[c]	2	2.21	2.36	1.75	1.86	1.80	1.80	1.43	1.39	1.39
		(1.3)	(1.2)	(4.4)	(1.9)	(3.1)	(3.1)	(1.5)	(2.0)	(1.0)
67.5	2	2.31	2.42	1.88	1.84	1.88	1.83	1.35	1.29	1.23
		(6.3)	(2.6)	(8.3)	(6.2)	(7.2)	(7.7)	(10.2)	(6.6)	(3.5)
90.6	1	2.07	2.03	1.98	1.97	1.66	1.71	1.59	1.33	1.33
100	5	2.14	2.20	1.68	1.75	1.63	1.63	1.09	1.07	1.10
		(10.0)	(6.9)	(4.3)	(5.6)	(4.9)	(6.0)	(6.6)	(5.9)	(8.1)
125	4	2.16	2.30	1.68	1.56	1.57	1.63	1.11	1.07	1.12
		(4.0)	(7.7)	(6.2)	(11.7)	(7.5)	(8.5)	(10.4)	(3.8)	(9.9)

[a] Number of determinations.
[b] Figures in parentheses represent precision (%).
[c] Measurement was made at room temperature (24°C).

thors excluded the data on the carbonyl carbon.[18]

Table VI summarizes the ^{13}C-T_1 data obtained from the NMR samples prepared at several test sites by each collaborator. Similarly to the corresponding ^1H-T_1 data, there is no substantial difference between the corresponding data in Tables IV and VI.

Longer T_1's in ^{13}C NMR at higher resonance frequencies may cause the great disadvantage of requiring longer delay time between rf pulses, resulting in decreased practical S/N ratio obtainable in a limited period of time, because ^{13}C NMR measurement usually needs more iterative accumulation than ^1H NMR measurement.

^{13}C Nuclear Overhauser Enhancement for PMMA

^{13}C NOE directly affects the signal intensities in ^{13}C NMR spectrum so that the assessment of the NOE data and its precision is desired for quantitative analysis. The NOE can also afford information on segmental motion of polymer chains together with T_1 data. Here NOE is defined as follows:

$$\text{NOE} = I/I_0$$

where I and I_0 are observed signal intensities with and without proton irradiation. The theoretically expected maximum value for NOE is 2.988 if the ^{13}C nuclear megnetization relaxes through dipolar interaction with ^1H nucleus. I_0 was determined from the spectrum obtained under gated decoupling without NOE.

In Tables VII and VIII are summarized the individual data and mean values of NOE, respectively. Precision of NOE is as good as that of ^{13}C-T_1. NOE's obtained at or below 25 MHz are about 2.5–2.8 and close to their theoretically expected maxima for all but carbonyl carbons. NOE values decrease with increasing magnetic field strength as seen in Figures 4 and 5. This is another disadvantage for measuring the spectrum of high S/N ratios

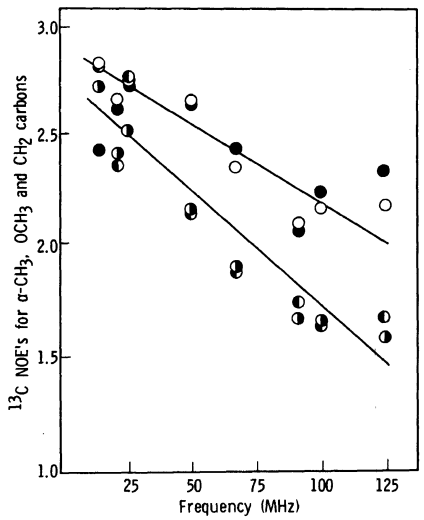

Figure 4. Frequency dependence of ^{13}C NOE's for α-CH_3, OCH_3, and CH_2 carbons of PMMA measured in $CDCl_3$ at 55°C: ○, α-CH_3 (*rr*); ●, α-CH_3 (*mr*); ◐, CH_2; ◑, OCH_3.

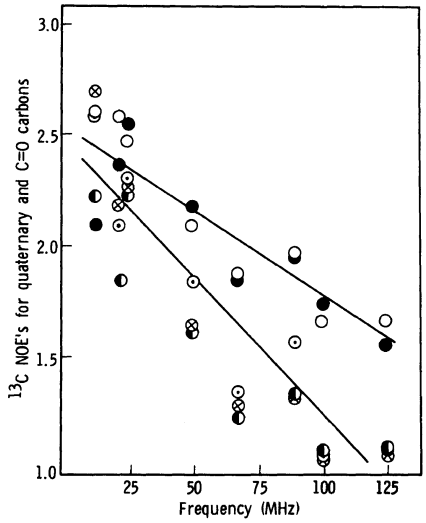

Figure 5. Frequency dependence of ^{13}C NOE's for quaternary and carbonyl carbons of PMMA measured in $CDCl_3$ at 55°C: ○, quaternary (*rr*); ●, quaternary (*mr*); ◐, carbonyl (*rrrm*); ⊙, carbonyl (*mmrr*+*rmrr*); ⊗, carbonyl (*rrrr*).

Table IX. Relative intensities of ^{13}C NMR signals of PMMA in $CDCl_3$ at 55°C[a]

Frequency	Complete decoupling[b]				Corrected by NOE[b]				Complete decoupling without NOE			
MHz	A	B	C	n[c]	A	B	C	n[c]	A	B	C	n[c]
22.5	0.86	1.93	1.00	3	1.11	2.15	1.07	3	1.12	2.21	1.19	2
25	0.86	2.00	1.00	3	1.04	2.07	1.08	3	0.97	2.00	1.03	1
50	0.54	1.45	0.92	3	0.87	1.80	1.14	3	0.89	2.00	1.03	1
67.5	0.55	1.52	0.75	1	1.01	1.94	0.96	1	0.99	1.95	1.02	2
90.6	0.43	1.33	0.70	1[d]	0.62	1.61	0.72	1[d]	—	—	—	—
100	0.33	1.54	0.67	1[d]	0.66	2.05	0.84	1[d]	1.00	2.06	1.08	2
100	0.46	1.33	0.69	1[e]	0.92	1.67	0.92	1[e]				
125	0.48	1.58	0.83	1[e]	0.97	2.20	1.14	1[e]	0.94	2.10	1.18	3

[a] A=C=O/α-CH_3, B=(CH_2+OCH_3)/α-CH_3, C=C-4/α-CH_3.
[b] Data except for e were taken from the previous paper.[1]
[c] Number of determinations.
[d,e] Pulse repetition times were *ca.* 1 s and 10 s, respectively.

by higher magnetic field instruments.

It is worth noting that the quaternary carbon, which has no directly attached hydrogens, shows similar NOE values to those for other carbons having directly attached hydrogens as CH_2 and CH_3 carbons. ^{13}C spin-lattice relaxation of the quaternary carbon seems to be governed mainly by dipole–dipole interaction with its neighboring protons in methyl and methylene groups. The carbonyl carbon shows distinctively lower NOE values than other carbons and the value comes close to unity at higher observing frequencies of 100 and 125 MHz. Compared at each frequency,

NOE for each carbon decreases in the order of α-CH_3>quaternary carbon$\simeq OCH_3 \simeq CH_2$>carbonyl carbon. The differences between NOE values of these carbons increase with increasing resonance frequency as seen in Figures 4 and 5, leading to inaccurate intensity ratios in completely decoupled spectra obtained at higher observing frequencies.

In the previous paper,[1] intensity ratios in ^{13}C NMR signals of the PMMA measured at 90.6 MHz and higher observing frequencies were reported to deviate from their theoretical values even after corrected by NOE values. The deviation was ascribed to the shorter repetition time of rf pulse (*ca.* 1 s). The intensity measurements were repeated at 100 and 125 MHz with a pulse repetition time of 10 s to avoid saturation of signals which would arise from longer ^{13}C-T_1 at higher magnetic fields. The data obtained are shown in Table IX along with the previously reported data. Through correction by the NOE values, the intensity ratios measured at 100 and 125 MHz with the repetition time of 10 s agreed well with the theoretically expected values. The average values of the intensity ratios determined from the spectra taken under the gated decoupling without NOE are also listed in the table and exhibit a good agreement with the theoretically expected values.

Acknowledgement. The authors are grateful to Mrs. F. Yano of Osaka University for her clerical assistance in preparing this manuscript.

REFERENCES

1. R. Chûjô, K. Hatada, R. Kitamaru, T Kitayama, H. Sato, and Y. Tanaka, *Polym. J.*, **19**, 413 (1987).
2. F. Horii, M. Nakagawa, R. Kitamaru, and members of NMR Research Group, SPSJ, *Polym. Prepr., Jpn.*, **36**, 3151 (1987).
3. K. Hatada, Y. Okamoto, K. Ohta, and H. Yuki, *J. Polym. Sci., Polym. Lett. Ed.*, **14**, 51 (1976).
4. K. Hatada, H. Ishikawa, T. Kitayama, and H. Yuki, *Makromol. Chem.*, **178**, 2753 (1977).
5. K. Hatada, T. Kitayama, Y. Okamoto, K. Ohta, Y. Umemura, and H. Yuki, *Makromol. Chem.*, **179**, 485 (1978).
6. F. Heatley and M. K. Cox, *Polymer*, **21**, 381 (1980).
7. F. Heatley and M. K. Cox, *Polymer*, **22**, 190 (1981).
8. J. Zajicek, H. Pivcová, and B. Schneider, *Makromol. Chem.*, **182**, 3169 (1981).
9. J. Zajicek, H. Pivcová, and B. Schneider, *Makromol. Chem.*, **182**, 3177 (1981).
10. J. R. Lyerla Jr., and T. T. Horikawa, *J. Polym. Sci., Polym. Lett. Ed.*, **14**, 641 (1976).
11. J. R. Lyerla, Jr., T. T. Horikawa, and D. E. Johnson, *J. Am. Chem. Soc.*, **99**, 2463 (1977).
12. Y. Inoue, T. Konno, R. Chûjô, and A. Nishioka, *Makromol. Chem.*, **178**, 2131 (1977).
13. Y. Inoue and T. Konno, *Makromol. Chem.*, **179**, 1311 (1978).
14. J. Spevácek and B. Schneider, *Polymer*, **19**, 63 (1978).
15. G. C. Levy and D. Wang, *Macromolecules*, **19**, 1013 (1986).
16. A. Abragam, "The Principles of Nuclear Magnetism," Oxford University Press, London and New York, 1961, Chapter 8.
17. G. C. Levy, J. P. Cargioli, and F. A. L. Anet, *J. Am. Chem. Soc.*, **95**, 1527 (1973).
18. G. C. Levy and D. Wang, *Macromolecules*, **19**, 1013 (1986).